Asian Journal of Chemistry; Vol. 38, No. 1 (2026), 215-222
ASIAN JOURNAL OF CHEMISTRY
https://doi.org/10.14233/ajchem.2026.34735

Design, Synthesis, Characterization and Molecular Docking Evaluation of Dual-Imino Benzopyran Analogues as Potential VEGFR2 and EGFR Inhibitors for Breast Cancer Therapy

Y. MANOGARAN[1], S. FULORIA[1,*], S. KARUPIAH[1], V. RAVICHANDRAN[1], V. BALAKRISHNAN[2] and N.K. FULORIA[1]

[1]Faculty of Pharmacy, AIMST University, Bedong 08100, Kedah, Malaysia
[2]Institute for Research in Molecular Medicine, Universiti Sains Malaysia, 11800 Pulau Pinang, Malaysia

*Corresponding author: E-mail: shivkanya_fuloria@aimst.edu.my

Received: 10 August 2025 *Accepted*: 15 December 2025 *Published online*: 31 December 2025 AJC-22241

The side effects associated with currently available chemotherapeutics for breast cancer treatments, intended present study to perform synthesis, characterization and molecular docking of novel benzopyrone analogues (NBPAs) against VEGFR2 (PDB: 6GQO) and EGFR (PDB: 3W32). The study involved the synthesis of some novel benzopyran analogues (NBPAs) by first treating 4-aminoacetophenone with a hydrazide derivative **5** of substituted benzopyrone (**1**), followed by treatment with different aromatic aldehydes to offer NBPAs (**6a-e**). NBPAs were characterized using ATR-IR, NMR (^{1}H & ^{13}C) and mass spectrometric analysis. The NBPAs were also subjected to molecular docking studies (using AutoDock 4.2) against VEGFR2 and EGFR. The results of the synthesis experiment and characterization study revealed successful synthesis of NBPAs and their structural elucidation. The docking study results also revealed NBPAs exhibit good binding affinity with 6GQO and 3W32. NBPAs exhibits good binding affinity against the targeted proteins 6GQO and 3W32. Present study concludes that synthesized novel NBPAs to exhibit high anticancer potential; however additional pre-clinical investigations are essential to support their clinical importance.

Keywords: Safety, Imino derivatives, Benzopyran derivatives, Anticancer activity, Docking studies.

INTRODUCTION

Current era witnessed incredible biological and chemical properties of coumarins [1,2]. The coumarins are known to comprise fused oxygenated heterocyclic ring called 1-benzopyran-2(2*H*)-one [3,4]. Benzopyrans were first time synthesized in midst of 19th century with the breakthrough of Perkin's reaction between salicylaldehyde and acetic anhydride [5]. Studies states that benzopyrans attributed to their basic nature undergoes non-covalent interactions with various receptors in living organisms and exerts several therapeutic actions [4-7]. According to multiple investigations, breast cancer is the primary cause of death among women [8]. It was estimated about 0.29 million new breast cancer cases by year 2023 and it will further exceed 3 million cases by year 2040, accompanied by around 1 million deaths [9]. While the majority of breast cancer cases are diagnosed at an early stage, 20-30% of patients experience distant recurrence, where cancer cells migrate to other body regions [10]. Breast cancer is commonly linked with risk factors, including genetics, aging, reproductive factors, lifestyle and hormonal imbalances [11]. Although chemotherapy and hormonal therapy are generally used to treat breast cancer, the significant adverse effects and the development of resistance cause the treatments to become ineffective, posing a major challenge for healthcare professionals [12]. This highlights the vitalness of identifying more selective and effective agents for breast cancer treatment.

Benzopyran scaffold holds great significance for medicinal chemists from the therapeutic perspective, as it exhibits significant anticancer properties by targeting and inhibiting various critical signalling pathways and enzymatic systems [13]. Some investigations have also shown that introducing an imino group into an organic moiety can improve its anticancer activity [14]. A previous study demonstrated that introducing a single imino group into the benzopyran moiety enhanced its cytotoxic effects against breast cancer cells (MCF-7) and revealed safety toward normal HEK-293 cells [15]. However, the study by Manogaran *et al.* [15] was limited to examining only single imino group and lacked supportive molecular docking data to evaluate binding affinity to EGFR and VEGFR2 receptors. These limitations prompted the current investigation to explore the impact of incorporating two

This is an open access journal, and articles are distributed under the terms of the Attribution 4.0 International (CC BY 4.0) License. This license lets others distribute, remix, tweak, and build upon your work, even commercially, as long as they credit the author for the original creation. You must give appropriate credit, provide a link to the license, and indicate if changes were made.

imino groups into the benzopyran structure. The objective was to synthesise, characterise new benzopyran analogues (NBPAs, **6a-e**) and molecular docking studies to analyse their interactions with EGFR and VEGFR2 receptors. This study aims to determine whether dual imino substitution enhances anticancer efficacy and receptor binding and compares its findings with the results of Manogaran *et al.* [15].

EXPERIMENTAL

The chemicals required for the synthesis of novel benzopyran analogues (NBPA) were acquired by Sigma-Aldrich, Friendemann-Schmidt, Merck-KGaA, HmbG-Chemicals and Qrec Chemicals. The synthesized NBPAs (**6a-e**) were characterized with (^{1}H & ^{13}C) NMR spectroscopy recorded on a Bruker spectrometer operating at 400 MHz. The IR spectra were captured on a ATR-IR spectrometric (ranging from 4000-400 cm^{-1}) and mass spectrometric data was generated from a Direct Infusion Ion Trap Mass analyzer. The synthesized NBPAs purity was analyzed by the SMP11 Analogue device. The reactions were observed through TLC analysis), utilizing solvent mixture of CH_3OH:$CHCl_3$ (3:2) [16].

Synthesis of *N*-(1-(4-aminophenyl)ethylidene)-2-(2-oxo-2*H*-chromen-4-yloxy)acetohydrazide (5): The synthesis of NBPA **5** was done using established method with minor adjustments [16,17]. Briefly, the substituted hydrazide **3** (0.0001 M) was synthesized by hydrazination of chromen-4-yloxy ester (**2**) obtained from 4-hydroxy coumarin (**1**) and then refluxed with 4-aminoacetophenone (0.0001 M) in absolute ethanol for 8 h at 78 ºC. Crude product was subjected to recrystallization using methanol, to yield pure NBPA **5** (**Scheme-I**). Brownish-yellow crystals, yield: 80%, m.p.: 60 ºC, R_f: 0.31; FT-IR (ATR, cm^{-1}): 3389 & 3329 (N–H primary), 3223 (N–H secondary), 3083 (=C–H), 2948 (C–H), 1648 (O=C), 1587 (C=N); ^{1}H NMR (DMSO-d_6, δ ppm): 1.03 (s, 3H, CH_3), 3.57 (s, 2H, OCH_2), 5.09 (s, 1H, C–H of pyran), 5.91 (NH_2), 6.53-7.66 (m, 8H, Ar-H), 9.99 (s, ^{1}H, NH-N); ^{13}C NMR (DMSO-d_6, δ ppm): 26 (CH_3), 65 (O-CH_2), 72 (=C–H), 103, 105, 113, 115, 117, 119, 121, 123, 125, 127, 129, 131, 136, 137, 139, 144, 151, 154 (Ar–C), 155 (N=C),162 (N=C of hydrazone), 164 (O=C of pyran), 166 (=C of pyran), 191 (O=C–NH); mass (*m/z*): 351 (M^+ signal).

Synthesis of N-(1-(4-(substituted benzylideneamino)-phenyl)ethylidene)-2-(2-oxo-2*H*-chromen-4-yloxy)aceto-hydrazide (6a-e): The synthesis of novel NBPAs **6a-e** was done using established method with minor adjustments [18]. Briefly, NBPA **5** (0.0001 M) was refluxed with 4-chlorobenzaldehyde (0.0001 M) in absolute ethanol for 6 h at 78 ºC. Crude product was subjected to recrystallization using methanol, to yield pure compound **6a**. The similar protocol was followed to synthesize the remaining compounds **6b-e** (**Scheme-I**).

***N*-(1-(4-(2-Chlorobenzylideneamino)phenyl)ethylidene)-2-(2-oxo-2*H*-chromen-4-yloxy)acetohydrazide (6a):** Yellow crystals, yield: 78%, m.p.: 136.2 ºC, R_f: 0.52; FT-IR (ATR, cm^{-1}): 3213 (N–H), 3044 (=C–H), 2928 (C–H), 1648 (O=C), 1595 (C=N); ^{1}H NMR (DMSO-d_6, δ ppm): 1.04 (s, 3H, CH_3), 3.58 (s, 2H, OCH_2), 5.57 (s, 1H, C–H of pyran), 6.54-7.78 (m, 12H, Ar-H), 9.33 (s, 1H, N=CH) and 10.33 (s, 1H, NH–N); ^{13}C NMR (DMSO-d_6, δ ppm): 26 (CH_3), 65 (O-CH_2), 72 (=C–H), 103, 105, 113, 115, 117, 119, 121, 123, 125, 127, 129, 131, 136, 137, 139, 144, 151, 154 (Ar–C), 155 (N=C), 162 (N–N=C of hydrazone), 164 (O=C of pyran), 166 (=C of pyran), 191 (NH–C=O); Mass (*m/z*): 473 (M^+ signal) and 475 (M+2 signal).

***N*-(1-(4-(4-Hydroxybenzylideneamino)phenyl)ethylidene)-2-(2-oxo-2*H*-chromen-4-yloxy)acetohydrazide (6b):** Reddish-orange crystals, yield: 73%, m.p.: 35.3 ºC, R_f: 0.41; FT-IR (ATR, cm^{-1}): 3319 (O–H), 3213 (N–H), 3044 (=C–H), 2923 (C–H), 1648 (O=C), 1588 (C=N); ^{1}H NMR (DMSO-d_6, δ ppm): 1.04 (s, 3H, CH_3), 3.57 (s, 2H, OCH_2), 5.60 (s, 1H, C–H of pyran), 6.47-7.76 (m, 12H, Ar–H), 9.76 (s, 1H, N=CH) and 10.22 (s, 1H, NH–N); ^{13}C NMR (DMSO-d_6, δ ppm): 26 (CH_3), 66 (O–CH_2), 74 (=C–H), 91, 113, 116, 117, 119, 123, 124, 125, 127, 129, 131, 133, 152 (Ar–C), 154 (N=C), 162 (N=C of hydrazone), 166 (O=C of pyran), 195 (NH–C=O); mass (*m/z*): 455 (M^+ signal).

***N*-(1-(4-(4-Dimethylamino-benzylideneamino)phenyl)-ethylidene)-2-(2-oxo-2*H*-chromen-4-yloxy)acetohydrazide (6c):** Dark red crystals, yield: 82%, m.p.: 58.1 ºC, R_f: 0.36; FT-IR (ATR, cm^{-1}): 3214 (N–H), 3044 (=C–H), 2923 (C–H), 1645 (O=C), 1590 (C=N); ^{1}H NMR (DMSO-d_6, δ ppm): 1.00 (s, 3H, CH_3), 2.79 (s, 6H, CH_3), 3.57 (s, 2H, OCH_2), 5.56 (s, 1H, C–H of pyran), 6.54-7.68 (m, 12H, Ar–H), 9.64 (s, 1H, N=CH) and 9.99 (s, 1H, NH–N); ^{13}C NMR (DMSO-d_6, δ ppm): 26 (CH_3), 40 ($N(CH_3)_2$) 60 (O–CH_2), 74 (=C–H), 103, 105, 113, 115, 117, 119, 121, 123, 125, 127, 129, 131, 136, 137, 139, 144, 151, 154 (Ar–C), 155 (N=C), 162 (N=C of hydrazone), 164 (O=C of pyran), 166 (=C of pyran), 192 (NH–C=O); Mass (*m/z*): 482 (M^+ signal).

***N*-(1-(4-(4-Chlorobenzylideneamino)phenyl)ethylidene)-2-(2-oxo-2*H*-chromen-4-yloxy)acetohydrazide (6d):** Light yellow crystals, yield: 76%, m.p.: 148.4 ºC, R_f: 0.58; FT-IR (ATR, cm^{-1}): 3213 (N–H), 3043 (=C–H), 2927 (C–H), 1646 (O=C), 1597 (C=N); ^{1}H NMR (DMSO-d_6, δ ppm): 1.04 (s, 3H, CH_3), 3.59 (s, 2H, OCH_2), 5.52 (s, 1H, C–H of pyran), 6.44-7.93 (m, 12H, Ar–H), 9.58 (s, 1H, N=CH) and 10.18 (s, 1H, NH-N); ^{13}C NMR (DMSO-d_6, δ ppm): 26 (CH_3), 65 (O-CH_2), 72 (=C–H), 103, 105, 113, 115, 116, 119, 121, 123, 125, 128, 129, 130, 133, 135, 139, 140, 144, 152 (Ar-C), 154 (N=C), 161 (N=C of hydrazone), 164 (O=C of pyran), 167 (=C of pyran), 192 (NH-C=O); mass (*m/z*): 473 (M^+ signal).

***N*-(1-(4-(2-Hydroxybenzylideneamino)phenyl)ethylidene)-2-(2-oxo-2*H*-chromen-4-yloxy)acetohydrazide (6e):** Dark yellow crystalline, yield: 80%, m.p.: 70.2 ºC, R_f: 0.46; FT-IR (ATR, cm^{-1}): 3394 (O-H), 3214 (N–H), 3044 (=C–H), 2927 (C–H), 1648 (O=C), 1588 (C=N); ^{1}H NMR (DMSO-d_6, δ ppm): 1.21 (s, 3H, CH_3), 3.57 (s, 2H, OCH_2), 5.59 (s, 1H, C–H of pyran), 6.54-7.75 (m, 12H, Ar–H), 8.30 (s, 1H, N=CH) and 10.22 (s, 1H, NH–N); ^{13}C NMR (DMSO-d_6, δ ppm): 26 (CH_3), 65 (O–CH_2), 72 (=C–H), 104, 107, 113, 115, 116, 119, 122, 124, 125, 129, 131, 136, 144, 125, 154 (Ar-C), 155 (N=C), 161 (N=C of hydrazone), 164 (O=C of pyran), 167 (=C of pyran), 191 (NH–C=O); mass (*m/z*): 455 (M^+ signal).

Molecular docking analysis: Modelling software Chem Office-16, Discovery Studio Visualizer 3.0, Swiss Protein Data Base Viewer, PyRx and AutoDock 4.2, was used in present study [19]. Proteins 3D structure such as Human

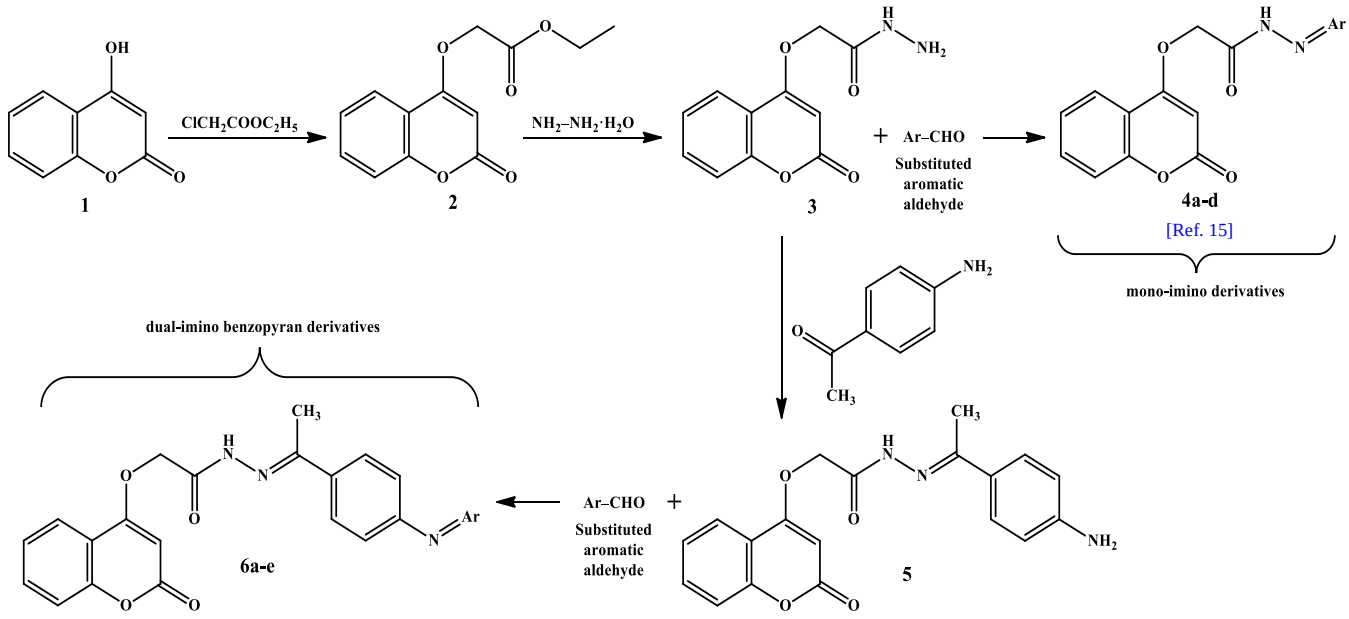

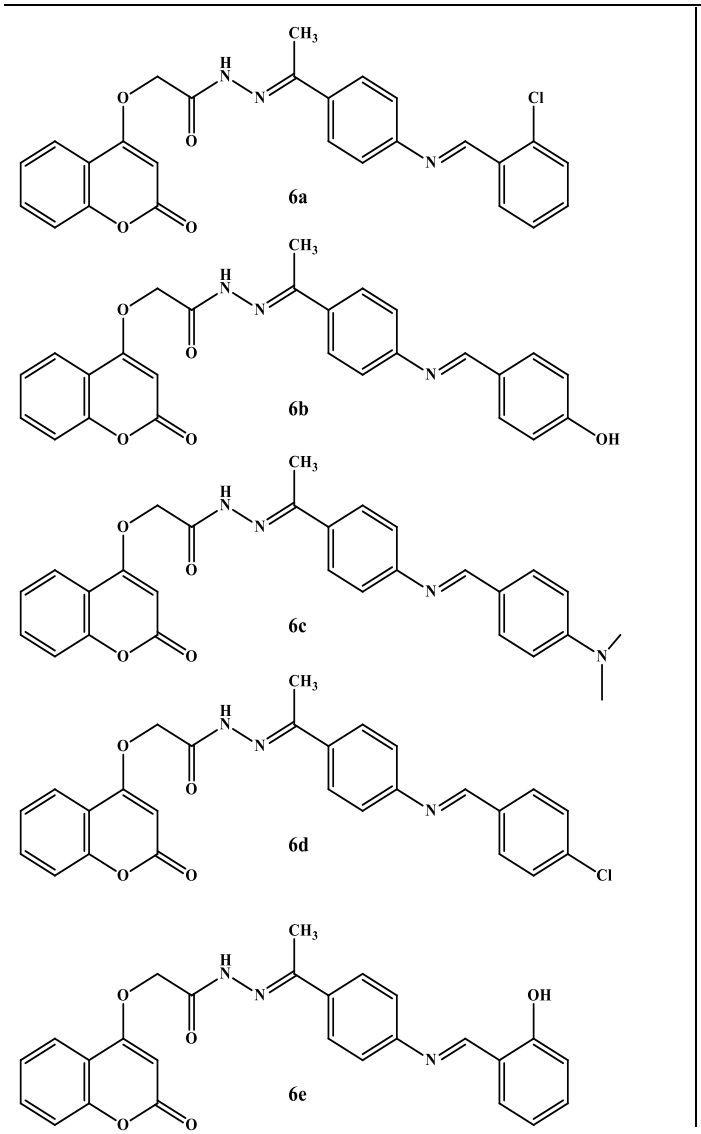

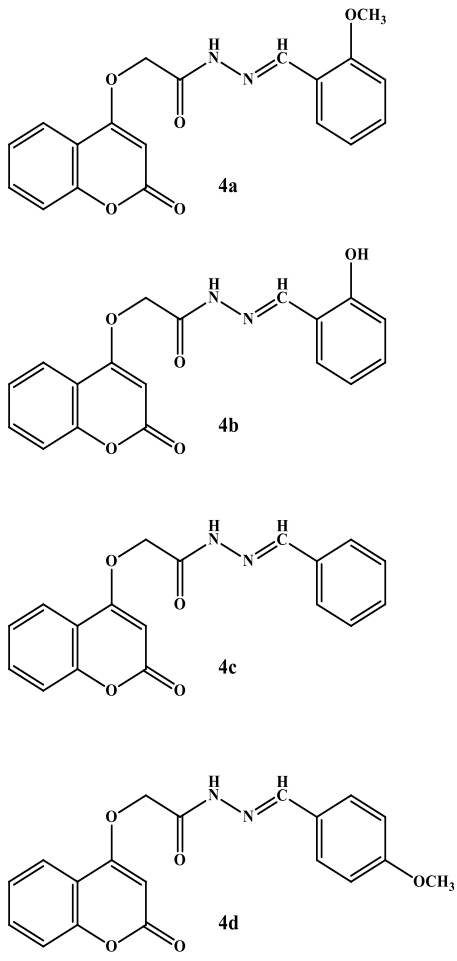

Scheme-I: Synthetic route of novel NBPAs (**6a-e**)

KDR (VEGFR2) Kinase domain (6GQO) and EGFR Kinase domain (3W32) were obtained from protein data bank (PDB) [20,21].

In present study, the NBPAs (including compound **4a-d** synthesized in previous study of Manogaran *et al.* [15] were further assessed for their interaction and binding affinity with the target proteins VEGFR2 and EGFR (using PyRx and Autodock 4.2). The chemical structures of all NBPAs were designed and modelled using Chemdraw 2D software. For molecular docking analysis, designed structures of NBPAs were optimized, followed by energy minimization using Chemdraw 3D and AutoDock software [22-26]. Preparation of receptors involved different steps such as removing heteroatoms (water and ions), incorporating polar hydrogen and assigning charges. Active sites were defined with the bounds of co-crystal ligands within grid boxes of a relevant dimension. The virtual screening was conducted using PyRx for visualization, then docking with Autodock 4.2 [19]. The docked pose of ligands and their interactions were analysed at the end of molecular docking analysis. The docked results were analysed by Discovery Studio Visualizer.

RESULTS AND DISCUSSION

Based upon established literature method [27] and extending our earlier work on the synthesis of mono-imino derivatives of 4-hydroxycoumarin (**4a-d**) [15], the present study was strategically designed to develop a new class of dimer-imino derivatives of 4-hydroxycoumarin. The synthetic strategy, outlined in **Scheme-I**, enabled the efficient construction of nitrogen-bridged pharmacologically active scaffolds (NBPAs), delivering compounds **5** and **6a-e** in consistently good yields. This approach not only demonstrates the synthetic versatility of the 4-hydroxycoumarin framework but also provides access to structurally complex dimeric architectures with enhanced potential for biological activity.

In present study, initally compound **3** was treated with 4-aminoacetophenone to form monomeric derivative **5**, which was further treated with various aromatic aldehyde to form dimeric imino derivatives (**6a-e**) using Schiff reaction. The synthesis of NBPAs took place under anhydrous conditions and was purified by recrystallization in hot methanol and activated charcoal. NBPAs purity was assessed based on their distinct melting point and single spot TLC pattern. The structural characterization of the synthesized NBPAs (**5** and **6a-e**) was supported by IR, NMR and mass spectrometric analyses. The IR spectra exhibited bands between 1587 and 1597 cm^{-1} related to C=N stretching vibration. In ^{1}H NMR spectra, signals in the δ 8.30-9.76 ppm range were attributed to the N=CH protons, while the ^{13}C NMR spectra displayed peaks around δ 161-162 ppm, indicative of the N-N=C carbon atoms. Molecular ion peaks observed in the mass spectra at *m/z* values of 473, 455, 482, 473 and 455 for compounds **6a-e**, respectively, further confirmed the proposed structures of the synthesized NBPAs.

Docking studies: The reliability of a molecular docking protocol is commonly validated by the root mean square deviation (RMSD) between the crystallographic ligand pose and the re-docked conformation, with values below 2 Å generally accepted as indicative of methodological accuracy [19]. In present study, re-docking of the native ligands into their respective binding sites of the crystallographic protein-ligand complexes yielded RMSD values of 0.255 Å and 1.721 Å. Both values fall well within the acceptable threshold, thereby confirming the robustness and validity of the docking protocol employed. The superimposed re-docking poses of the extracted ligands within the active sites of proteins 6GQO and 3W32 are illustrated in Fig. 1.

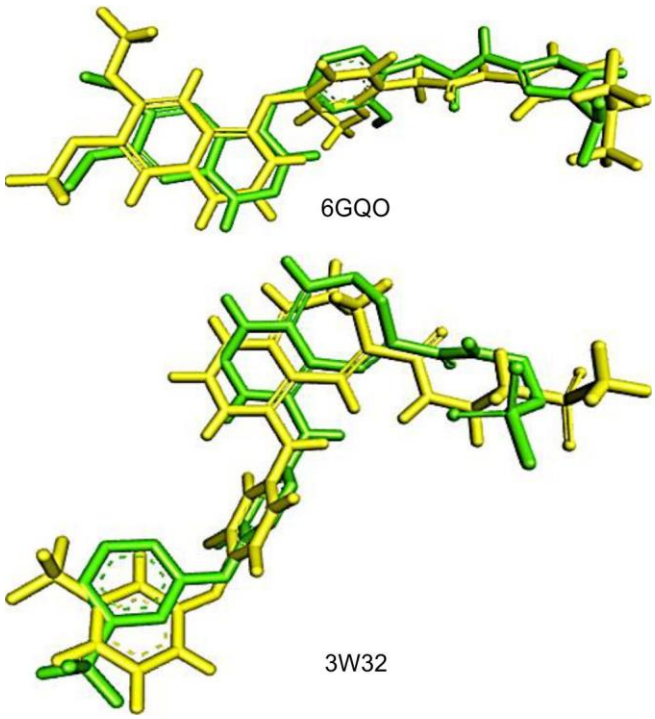

Fig. 1. Re-docking pose of the extracted ligands of 6GQO and 3W32

Virtual screening was done by using PyRx to narrow down the candidates, followed by AutoDock 4.2 to evaluate the binding affinity of NBPAs more accurately with the kinase domain of human KDR (VEGFR2) with PDB ID: 6GQO; and EGFR kinase domain with PDB ID: 3W32 [19,23,24,26]. The virtual screening of docking results (using PyRx) for all NBPAs (**5** and **6a-e**) and the prior synthesized compounds (**1**, **2**, **3** and **4a-d**) are presented in Table-1. All compounds exhibited strong binding affinity (inhibition) by fully occupying the active sites of the target proteins 6GQO and 3W32. Next, among all the compounds, **6d** offering the highest binding energy was further subjected to molecular docking against 6GQO and 3W32 using AutoDock 4.2. Based on the AutoDock *in silico* data, the binding energy of **6d** with VEGFR2 is -12.83 kcal/mol and with EGFR is -11.41 kcal/mol (Table-2).

Based on the molecular docking analysis data for standard drug, axitinib with 6GQO (Fig. 2), it is revealed that 2D configuration of NBPA **6d** engaged in significant interactions with amino acids present in the human KDR kinase domain. Conventional hydrogen bonds formed between the 'O' atom of benzopyran ring in the standard drug and the aspartic acid of protein 6GQO. Moreover, 3D depiction of molecular docking analysis complex confirms existence of these interactions, offering further insights into the binding mode of

TABLE-1
BINDING ENERGY OF NBPAS AND PRIOR SYNTHESIZED COMPOUNDS WITH 6GQO AND 3W32 (USING Pyrx)

Compounds	Binding affinity (kcal/mol)	
	6GQO	3W32
1	-5.84	-6.30
2	-6.57	-6.71
3	-6.58	-6.90
4a	-8.61	-8.63
4b	-8.91	-8.49
4c	-8.11	-9.06
4d	-7.75	-9.61
5	-9.02	-8.64
6a	-10.91	-10.84
6b	-10.53	-8.62
6c	-10.19	-8.97
6d	-11.83	-10.87
6e	-10.57	-8.88

TABLE-2
BINDING ENERGY OF COMPOUND **6d** WITH 6GQO AND 3W32 (VALIDATION USING AutoDock 4.2)

Compound	Binding affinity (kcal/mol)	
	6GQO	3W32
6d	-12.83	-11.41
Axitinib	-12.77	–
Lapatinib	–	-12.18

axitinib within VEGFR2 Kinase domain's active site (Fig. 2). Moreover, conventional H-bonds also found between NO_2 group of standard drug and cysteine amino acid of protein. Conventional H-bonding between the standard drug and protein residues stabilizes complex and improves its binding affinity [28]. The 2D diagram shown in Fig. 2 demonstrates exact orientation of the standard drug within the protein's binding site.

Based on molecular docking analysis results of NBPA **6d** with 6GQO (Fig. 3), it is revealed that 2D configuration of NBPA **6d** engage in significant interaction with amino acids present in the human KDR (VEGFR2) kinase domain. Conventional hydrogen bonds are formed between oxygen atom of benzopyran ring in NBPAs **6d** and the amino acids of protein 6GQO (asparagine and arginine). Conventional hydrogen bonds also formed between the NH group of benzopyran ring in NBPA **6d**. These covalent hydrogen bonds are strong and stabilize the compound in the binding site. This covalent bonding is also vital for better orientation and tight anchoring of a ligand [29]. Moreover, 3D depiction of molecular docking analysis complex confirms existence of these interactions, offering further insights into the binding mode of NBPA **6d** within VEGFR2 Kinase domain's active site (Fig. 3).

Furthermore, the pi-pi stacked interactions were found between phenylalanine with the aromatic rings of NBPA **6d**. The pi-cation interaction is also found between aromatic ring of NBPA **6d** and lysine amino acid of protein 6GQO. These interaction further stabilizes the ligand structure *via* electrostatic interaction [30]. Furthermore, alkyl interaction (hydrophobic interaction) were observed between the NBPA **6d** and amino acids of protein 6GQO (valine, leucine, alanine, lysine, cysteine) which contributes in hydrophobic stabilization by fitting the NBPA **6d** into non-polar binding pocket of protein 6GQO [31,32]. A pi-donor hydrogen bond interaction was observed between the aromatic ring of NBPA **6d** and a cysteine residue within the active site of protein 6GQO. The two-dimensional interaction map presented in Fig. 3 clearly illustrates the precise orientation and binding mode of NBPA **6d** within the protein binding pocket. The formation of stabilizing hydrogen-bond interactions with key amino acid residues suggests that NBPA **6d** may effectively interfere with the attachment of breast cancer cells to host cells, thereby contributing to its observed anti-breast cancer activity.

Based on the molecular docking analysis data for standard drug, lapatinib with 3W32 (Fig. 4), it is shown that the 2D configuration of the standard drug engaged in significant interaction with amino acids present in EGFR kinase domain. The conventional hydrogen bonds were further formed between fluorine atom of the benzopyran ring in

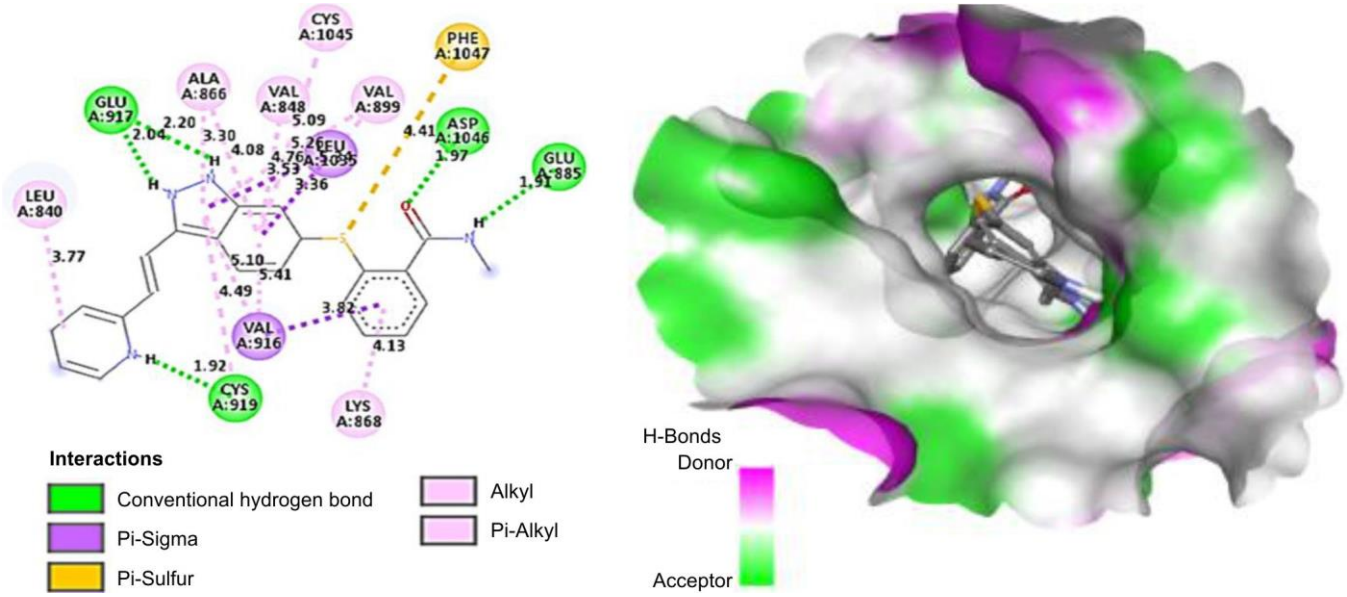

Fig. 2. 2D and 3D conformation poses of dock image of 6GQO with axitinib

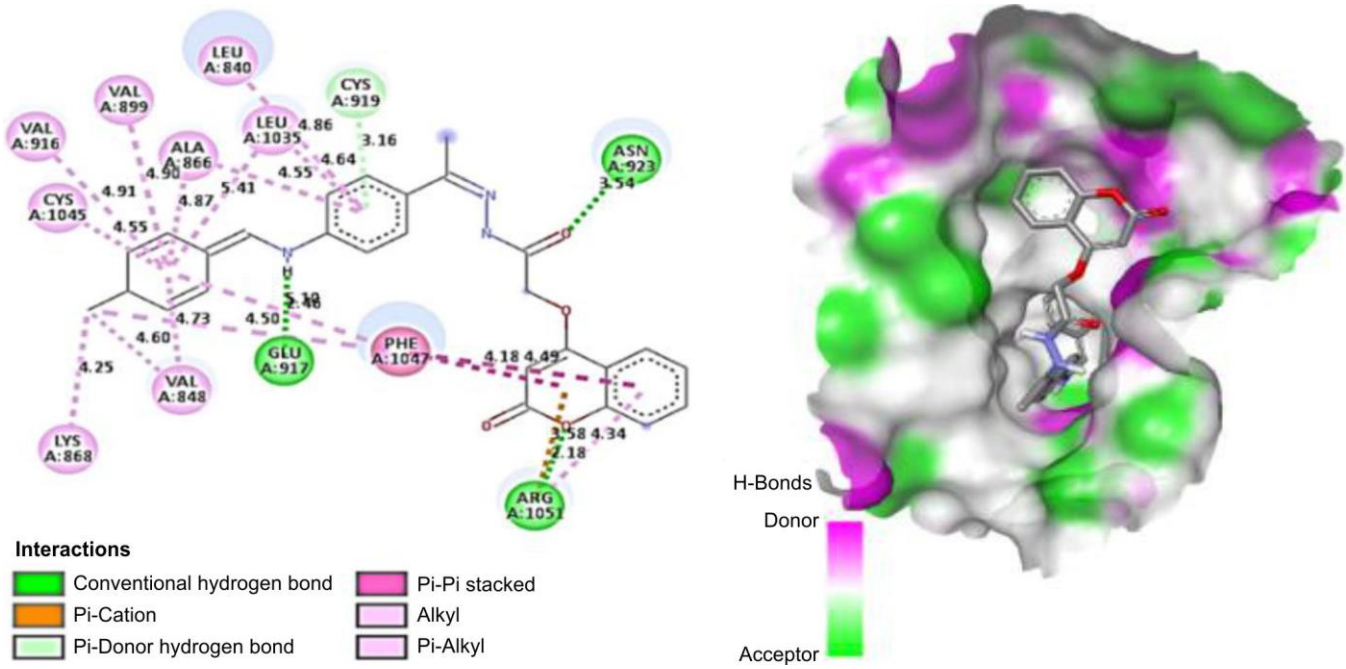

Fig. 3. 2D and 3D conformation poses of dock image of 6GQO with compound **6d**

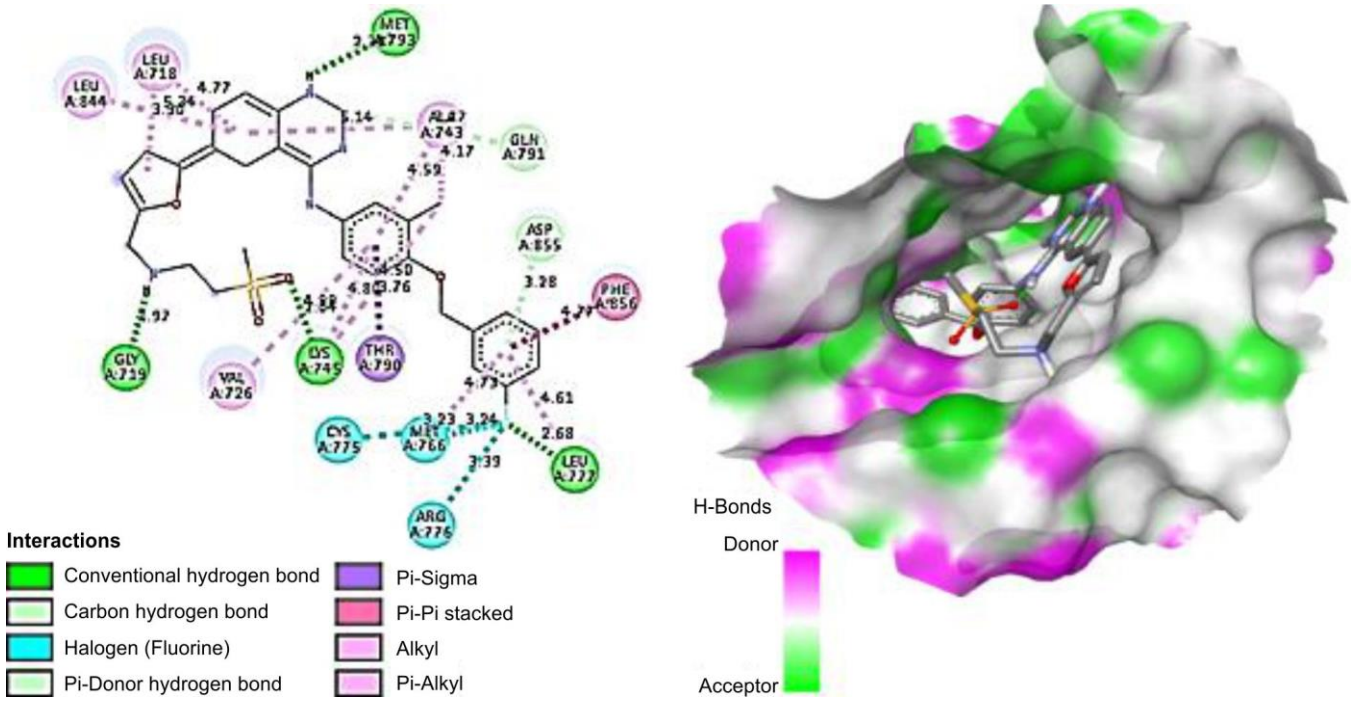

Fig. 4. 2D and 3D conformation poses of dock image of 3W32 with lapatinib

standard drug and leucine part of protein 3W32. Moreover, 3D depiction of molecular docking analysis complex proves existence of these interactions, offering further insights into the binding mode of lapatinib in active site of EGFR Kinase domain (Fig. 4). In addition, the conventional hydrogen bonds interactions also were observed between nitro group of the standard drug and methionine and glycine part of the protein. Conventional hydrogen bonds were formed between oxygen atom of benzopyran ring in standard drug and the lysine amino acid of protein 3W32. The conventional hydrogen bonding between standard drug and protein residues stabilizes complex and improves its binding affinity [28]. 2D diagram shown in Fig. 4, demonstrates exact orientation of the standard drug within the protein's binding site, emphasizing the particular H-bond interactions between ligand and protein residues.

According to the molecular docking analysis data for NBPA **6d** with 3W32 (Fig. 5), it revealed that NBPA **6d** also exhibited significant interaction with the amino acids in the (EGFR) kinase domain as well. Whereas the 3D model of the

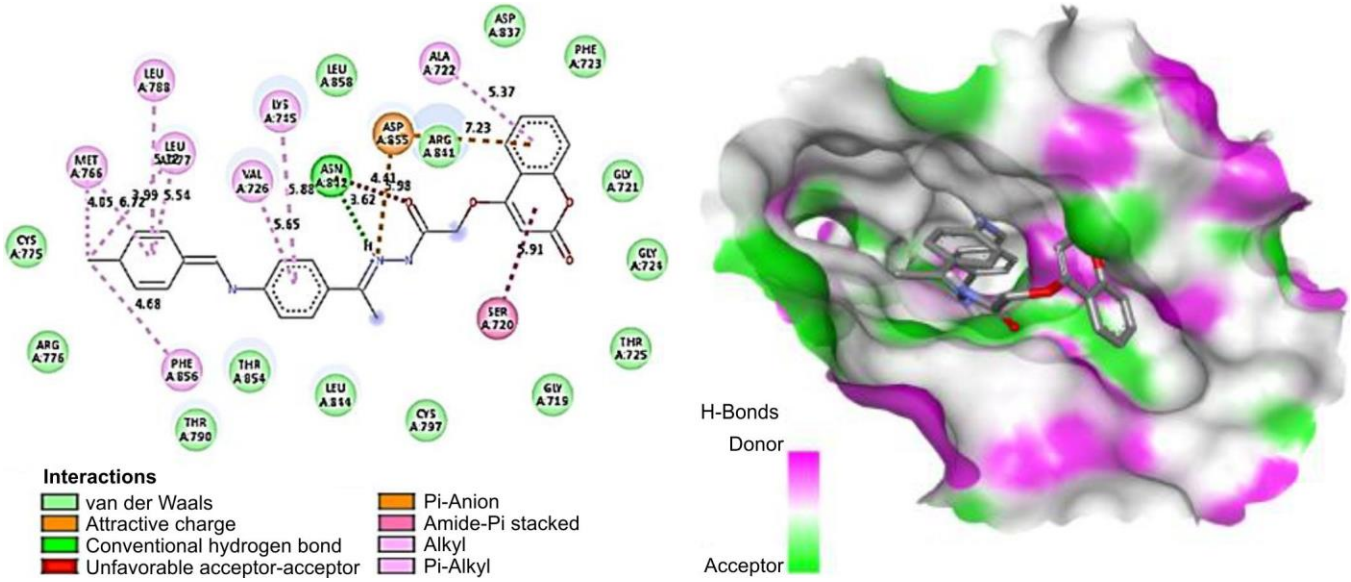

Fig. 5. 2D and 3D conformation poses of dock image of 3W32 with compound **6d**

molecular docking analysis complex offers further insights into binding mode of NBPA **6d** in the active site of EGFR kinase domain (Fig. 5). Conventional hydrogen bond was formed between NH-group of benzopyran ring in NBPA **6d** and the asparagine amino acid of protein 3W32. These covalent hydrogen bonds are strong and stabilizes the compound in the binding site. This covalent bonding is also vital for better orientation and tight anchoring of a ligand [29]. Furthermore, alkyl and pi-alkyl interactions (hydrophobic interaction) were observed between the NBPA **6d** and amino acids of protein 3W32 (valine, leucine, alanine, lysine, methionine and phenylalanine), which contributes hydrophobic stabilization by fitting NBPA **6d** into non-polar binding pocket of protein 6GQO [31,32]. The van der Waals interaction was observed between NBPA **6d** and the amino acids of protein 3W32 (cysteine, arginine, threonine, leucine, asparagine, phenylalanine and glycine). This interaction is vital for binding free energy [31]. The amide-pi stacked interaction was also observed between the aromatic ring of NBPA **6d** with serine amino acid of protein 3W32. This interaction provides orientation stability of NBPAs contributes to aromatic complementarity [33]. The pi-anion interaction was further observed between asparagine amino acid of protein 3W32 and NBPA **6d** (with aromatic ring and NH-group). This interaction is considered to be stronger than van der Waals as provides further stability to the NBPA **6d** [34]. The 3D depiction of molecular docking analysis confirms existence of these interactions, offering further insights into the binding mode of NBPA **6d** within EGFR active site (Fig. 5). 2D diagram (Fig. 5) demonstrates exact orientation of NBPA **6d** in protein's binding site. By forming H-bonds with essential amino acids in protein, NBPA **6d** may obstruct ability of breast cancer cells to attach to host cells, thus exhibiting anti-breast cancer properties.

Conclusion

This study reports the successful synthesis of novel benzopyrone analogues (NBPAs) from *N*-(1-(4-aminophenyl)ethylidene)-2-(2-oxo-2*H*-chromen-4-yloxy)acetohydrazide (**5**) *via* a Schiff base reaction. The structural confirmation of the synthesized NBPAs was achieved with IR, NMR and mass spectrometric data. The molecular docking analysis results of synthesized NBPAs demonstrated potential binding interactions with the kinase domain of human KDR (VEGFR2) and EGFR kinase domain. However, the synthesized NBPAs should be further subjected to pre-clinical testing to further confirm their effectiveness against breast cancer.

ACKNOWLEDGEMENTS

The authors are grateful to AIMST University, for its support in the successful completion of this study.

CONFLICT OF INTEREST

The authors declare that there is no conflict of interests regarding the publication of this article.

DECLARATION OF AI-ASSISTED TECHNOLOGIES

The authors declare that no AI tools were used in the preparation or writing of this research/review article.

REFERENCES

1. O. Firuzi, F. Borges, A. Gaspar, M. Mohabbati, F. Cagide, N. Razzaghi-Asl and R. Miri, *Res. Pharm. Sci.*, **14**, 74 (2019); https://doi.org/10.4103/1735-5362.251855
2. A.Y. Mohammed and L.S. Ahamed, *Chem. Methodol.*, **6**, 813 (2022); https://doi.org/10.22034/CHEMM.2022.349124.1569
3. E. Kupeli Akkol, Y. Genç, B. Karpuz, E. Sobarzo-Sánchez and R. Capasso, *Cancers*, **12**, 1959 (2020); https://doi.org/10.3390/cancers12071959
4. T.M. Pereira, D.P. Franco, F. Vitorio and A.E. Kummerle, *Curr. Top. Med. Chem.*, **18**, 124 (2018); https://doi.org/10.2174/1568026618666180329115523
5. J. Jumal and N. Sakinah, *Malays. J. Sci. Health Technol.*, **7**, 62 (2021); https://doi.org/10.33102/mjosht.v7i1.145
6. S. Losada-Barreiro, Z. Sezgin-Bayindir, F. Paiva-Martins and C. Bravo-Díaz, *Biomedicines*, **10**, 3051 (2022); https://doi.org/10.3390/biomedicines10123051

7. X.-M. Peng, G. L.V. Damu and C. He Zhou, *Curr. Pharm. Des.*, **19**, 3884 (2013); https://doi.org/10.2174/1381612811319210013
8. H. Sung, J. Ferlay, R.L. Siegel, M. Laversanne, I. Soerjomataram, A. Jemal and F. Bray, *CA Cancer J. Clin.*, **71**, 209 (2021); https://doi.org/10.3322/caac.21660
9. M. Arnold, E. Morgan, H. Rumgay, A. Mafra, D. Singh, M. Laversanne, J. Vignat, J.R. Gralow, F. Cardoso, S. Siesling and I. Soerjomataram, *Breast*, **66**, 15 (2022); https://doi.org/10.1016/j.breast.2022.08.010
10. H. Kennecke, R. Yerushalmi, R. Woods, M.C.U. Cheang, D. Voduc, C.H. Speers, T.O. Nielsen and K. Gelmon, *J. Clin. Oncol.*, **28**, 3271 (2010); https://doi.org/10.1200/JCO.2009.25.9820
11. T.O. Uhomoibhi, T.J. Okobi, O.E. Okobi, J.O. Koko, O. Uhomoibhi, O.E. Igbinosun, U.D. Ehibor, M.G. Boms, R.A. Abdulgaffar, B.L. Hammed, C. Ibeanu, E.O. Segun, A.A. Adeosun, E.O. Evbayekha and K.B. Alex, *Cureus*, **14**, e32309 (2022); https://doi.org/10.7759/cureus.32309
12. W.M.C. Van Den Boogaard, D.S.J. Komninos and W.P. Vermeij, *Cancers*, **14**, 627 (2022); https://doi.org/10.3390/cancers14030627
13. Y. Wu, J. Xu, Y. Liu, Y. Zeng and G. Wu, *Front. Oncol.*, **10**, 592853 (2020); https://doi.org/10.3389/fonc.2020.592853
14. M.A. Sa'ad, R. Kavitha, S. Fuloria, N.K. Fuloria, M. Ravichandran and P. Lalitha, *Antibiotics*, **11**, 207 (2022); https://doi.org/10.3390/antibiotics11020207
15. Y. Manogaran, S. Karupiah, V. Balakrishnan, N.K. Fuloria and S. Fuloria, *Asian J. Chem.*, **35**, 2948 (2023); https://doi.org/10.14233/ajchem.2023.30282
16. A.A. Siddiqui, R. Mishra and M. Shaharyar, *Eur. J. Med. Chem.*, **45**, 2283 (2010); https://doi.org/10.1016/j.ejmech.2010.02.003
17. M. Shaharyar, A. Mazumder, Salahuddin, R. Garg and R.D. Pandey, *Arab. J. Chem.*, **9**, S342 (2016); https://doi.org/10.1016/j.arabjc.2011.04.013
18. R. Kavitha, M.A. Sa'ad, S. Fuloria, N.K. Fuloria, M. Ravichandran and P. Lalitha, *Antibiotics*, **12**, 306 (2023); https://doi.org/10.3390/antibiotics12020306
19. R. Veerasamy and R. Karunakaran, *J. Genet. Eng. Biotechnol.*, **20**, 58 (2022); https://doi.org/10.1186/s43141-022-00339-y
20. T. Kar, P. Dugam, S. Shivhare, S.R. Shetty, S. Choudhury, D. Sen, B. Deb, S. Majumdar, S. Debnath and A. Das, *Cancer Rep.*, **7**, e2049 (2024); https://doi.org/10.1002/cnr2.2049
21. Z. Ruzi, K. Bozorov, L. Nie, J. Zhao and H.A. Aisa, *Biomed. Pharmacother.*, **156**, 113948 (2022); https://doi.org/10.1016/j.biopha.2022.113948
22. Z.M. Alamshany, R.R. Khattab, N.A. Hassan, A.A. El-Sayed, M.A. Tantawy, A. Mostafa and A.A. Hassan, *Molecules*, **28**, 739 (2023); https://doi.org/10.3390/molecules28020739
23. E. M. Hassan, Y. F. Mustafa, and M. M. Merkhan, *Int. J. Anal. Basic Appl. Sci.*, **6**, 1 (2022).
24. L. Cai, W. Liu, J.-F. Ning, W.-Q. Meng, J. Hu, Y.-B. Zhao and C. Liu, *Drug Des. Devel. Ther.*, **3837**, (2015); https://doi.org/10.2147/DDDT.S85357
25. A.T. McNutt, P. Francoeur, R. Aggarwal, T. Masuda, R. Meli, M. Ragoza, J. Sunseri and D.R. Koes, *J. Cheminform.*, **13**, 43 (2021); https://doi.org/10.1186/s13321-021-00522-2
26. F. Ramzan, S.A. Nabi, M.S. Lone, K. Imtiyaz, L. Urooj, V. Vishakha, K. Sharma, M.M.A. Rizvi, S. Shafi, M. Samim, S. Bano and K. Javed, *ACS Omega*, **8**, 6650 (2023); https://doi.org/10.1021/acsomega.2c07153
27. E. Hejchman, H. Kruszewska, D. Maciejewska, B. Sowirka-Taciak, M. Tomczyk, A. Sztokfisz-Ignasiak, J. Jankowski and I. Młynarczuk-Biały, *Monatsh. Chem.*, 150, 255 (2019); https://doi.org/10.1007/s00706-018-2325-5
28. D.A. Milenković, D.S. Dimić, E.H. Avdović and Z.S. Marković, *RSC Adv.*, **10**, 35099 (2020); https://doi.org/10.1039/D0RA07062A
29. M. Sako, N. Yasuo and M. Sekijima, *J. Chem. Inf. Model.*, **65**, 71 (2025); https://doi.org/10.1021/acs.jcim.4c01385
30. N. Wu, R. Zhang, X. Peng, L. Fang, K. Chen and J.S. Jestilä, *Phys. Chem. Chem. Phys.*, **26**, 6903 (2024); https://doi.org/10.1039/D3CP03492E
31. F. Molani and A.E. Cho, *Commun. Chem.*, **7**, 247 (2024); https://doi.org/10.1038/s42004-024-01328-7
32. M.A. Saragatsis, G.K. Kinsella, J.F. Curtin and T. Zhang, *ChemMedChem*, **20**, e202500365 (2025); https://doi.org/10.1002/cmdc.202500365.
33. L.M. Breberina, M.V. Zlatović, S.Đ. Stojanović and M.R. Nikolić, *Computation*, **12**, 172 (2024); https://doi.org/10.3390/computation12090172
34. Y. Khan, S. Iqbal, M. Shah, A. Maalik, R. Hussain, S. Khan, I. Khan, R.A. Pashameah, E. Alzahrani, A.-E. Farouk, M.I. Alahmdi and H.S.M. Abd-Rabboh, *Front Chem.*, **10**, 995820 (2022); https://doi.org/10.3389/fchem.2022.995820